Applied Catalysis A, General 619 (2021) 118158

Contents lists available at ScienceDirect

Applied Catalysis A, General

journal homepage: www.elsevier.com/locate/apcata

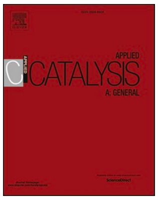

Flow reactor approach for the facile and continuous synthesis of efficient Pd@Pt core-shell nanoparticles for acceptorless dehydrogenative synthesis of pyrimidines from alcohols and amidines

Sharmin Sultana Poly [a,*], Yuta Hashiguchi [b], Asima Sultana [a], Isao Nakamura [a], Ken-ichi Shimizu [c], Shunsaku Yasumura [c], Tadahiro Fujitani [a,*]

[a] *Interdisciplinary Research Center for Catalytic Chemistry, National Institute of Advanced Industrial Science and Technology Tsukuba, Ibaraki 305-8565, Japan*
[b] *Research Association of High-Throughput Design and Development for Advanced Functional Materials, Tsukuba, Ibaraki, 305-8565, Japan*
[c] *Institute for Catalysis, Hokkaido University, N-21, W-10, Sapporo 001-0021, Japan*

ARTICLE INFO

Keywords:
Acceptorless dehydrogenative coupling
Multicomponent reaction
Pyrimidines
Flow reactor
Core-shell catalyst

ABSTRACT

Carbon supported Pd@Pt core-shell nanoparticles catalyst was prepared in a flow reactor toachieve enhanced catalytic activities with low Pt loading for the acceptorless dehydrogenative synthesis of pyrimidines. Spectroscopic (XAS analysis) and microscopic (HAADF-STEM) techniques reveled that the core-shell structure was formed by the applied preparation method. The Pd@Pt/PVP (polyvinylpyrrolidone)/C catalyst showed the activity for the three component one pot synthesis of pyrimidines through a series of consecutive reactions including oxidation of alcohols, C—C, and C—N coupling, followed by heterocyclization and dehydrogenation employing various primary alcohols, secondary alcohols, and amidines. The reaction mechanism on Pd@Pt/PVP/C catalyst was explored by comparison with the control experiments.

1. Introduction

Pyrimidines are important heterocycles in the synthesis of pharmaceuticals ingredients, agrochemicals, and various functional materials [1–3]. They have structural moieties as in natural products and biologically active molecules [4]. Pyrimidine is a key factor of some important drugs used for the treatment of hyperthyroidism, acute leukemia in children, and adult granulocytic leukemia [4–7]. In addition, several other pyrimidines show wide-spread pharmacological activities as antitumor, antibacterial, antifungal, antimalarial, analgesic, anticancer, and anti-cholesterol drug [5,8–18]. Therefore, the development of a green and sustainable method for the synthesis of pyrimidine derivatives from easily available starting materials is desired.

Over the past several decades, alcohols have been regarded as effective and inexpensive substrates transformed into value-added heteroatom-containing chemicals [19,20]. Among the transformations, H_2 evolving, acceptorless dehydrogenation (AD) reactions have become promising for eco-friendly C—C and C—N bond formation reactions using alcohols [21–41].

There are several reports of multicomponent reactions of heterocycles synthesis with variations in oxidants, solvents, and starting materials [42–46]. Transition metal based homogeneous catalysts have been utilized for synthetic processes related to fine chemicals, such as flavors and pharmaceuticals. Following these studies, several groups have recently reported new synthetic methods using the acceptorless dehydrogenative coupling (ADC) to obtain pyrimidines from easily available starting materials. The methods employ methodology. Kempe et al. [16,47] Kirchner et al. [48] Herbert et al. [49], Kundu et al. [50], Adhikari et al. [51] have reported the synthesis of pyrimidines through ADC condensation with a basic additive (KO*t*Bu) using homogeneous transition metal (such as Ir, Mn, and Ni) in one-pot multicomponent reaction. Very recently, Pt/C catalyst in a recyclable heterogeneous reaction system has been reported for the synthesis of pyrimidines from alcohols and amidines under ADC method [26]. Compared with the previous homogeneous catalytic system [14,34,47–51], the developed system achieved a high activity, higher turnover number (TON), a wide range of substrates scope and good reusability of the catalyst toward pyrimidine synthesis (Scheme 1).

To enhance the catalytic activity and reduce the usage of Pt, alloying Pt with Pd has been actively studied in several reports [52–67] and most

---

* Corresponding authors.
E-mail addresses: poly.sharmin@aist.go.jp (S.S. Poly), t-fujitani@aist.go.jp (T. Fujitani).

https://doi.org/10.1016/j.apcata.2021.118158
Received 24 February 2021; Received in revised form 4 April 2021; Accepted 12 April 2021

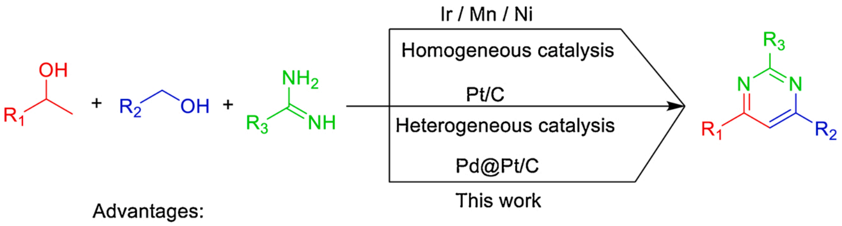

Advantages:

Preparation of Pd@Pt under continuous flow process

Precisely controlled particle size of metal NPs

Reduced the amount of noble metal

Scheme 1. Multi-component synthesis of pyrimidines.

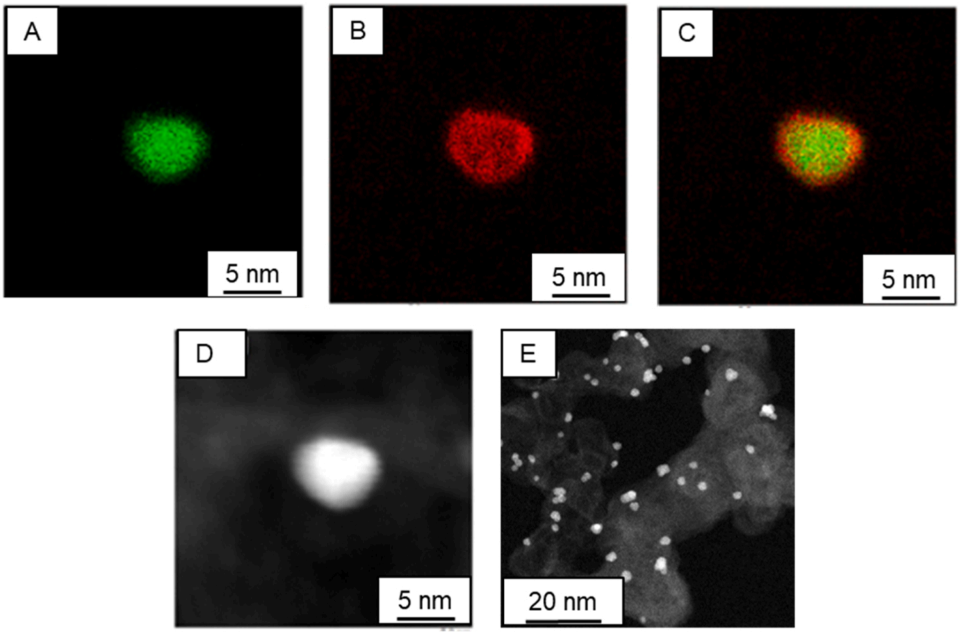

Fig. 1. DF-STEM-EDS mapping images (A-D), and DF-STEM image (E) with Pd shown in green and Pt in red, of Pd@Pt/PVP/C NPs synthesized by the flow process.

of the reported catalysts were found effective towards polymer electrolyte membrane fuel cells (PEMFC) [53,65,68–70]. In the present work, we design a bimetallic core-shell Pd@Pt/PVP (polyvinylpyrrolidone)/C catalyst was prepared in a flow reactor, resulting in a high efficiency and a synergistic effect between Pt and secondary metal Pd. The purpose of the PVP as a capping agent is to control the particle size and to prevent the agglomeration of nanoparticles [71–73]. Core-shell nanoparticles are also used as a template for the preparation of hollow particles after removing the core either by dissolution or calcination [74–76]. However, there are very few reports in organic synthesis with core-shell catalysts [77,78]. In this study, our challenge is to expand the uses of the core-shell catalyst for the synthesis of industrially important chemicals from multicomponent in a one pot manner. The high productivity of the desired heterocycle pyrimidines is a reflect of durability and high activity of synthesized bimetallic core-shell Pd@Pt/PVP/C catalyst with low loading of Pt and precisely control the nanoparticles particle size in flow reactor.

2. Results and discussion

2.1. Characterization of Pd@Pt/PVP/C

Pd@Pt core-shell NPs were synthesized using the flow-reactor process with K_2PdCl_4 as a Pd precursor, H_2PtCl_6 as a Pt precursor, $NaBH_4$ as a reductant, and polyvinylpyrrolidone as a capping agent with a total loading of Pd and Pt for 5 wt%. The details of the flow reactor and the preparation method of Pd@Pt/PVP/C catalyst are in experimental section (Fig. S1). Then the catalyst was characterized by various characterization techniques. To directly observe the core-shell structure of the supported nanoparticles, the dark field scanning transmission electron microscopy (DF-STEM) images were obtained, and elemental mapping with energy dispersive spectroscopy (EDS) was carried out. Fig. 1 shows STEM images for Pd@Pt/PVP/C samples. In this case, the edge of the sample was rich in Pt while the core was rich in Pd. From this result, we can conclude that the structure of core-shell catalyst Pd@Pt/PVP/C had been successfully synthesized.

Table 1
CO adsorption data of the catalysts pre-reduced at 300 °C.

Catalysts	Pt content (wt%)	Pd content (wt%)	Pt dispersion (%)	Surface area ($m^2 g^{-1}$)
Pt/C	5	0	11.93	29.46
Pd@Pt/PVP/C	2.5	2.5	12.65	31.24

The particle size of this Pd@Pt/PVP/C catalyst is 3.55 ± 0.62 nm (Fig. S2). Furthermore, from the results of electron energy loss spectroscopy (EELS) line analysis (Fig. S3), the thickness of the Pt shell was estimated to be approximately 0.5 nm, suggesting that the Pt shell

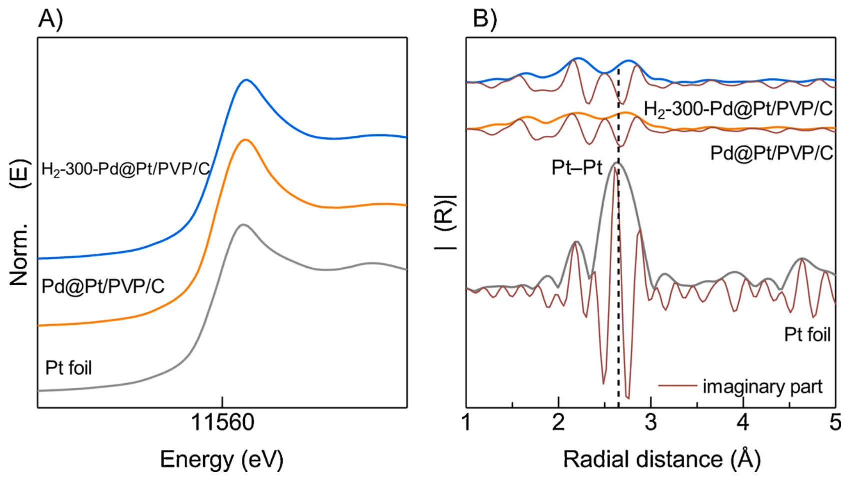

Fig. 2. Pt L_3-edge (A) XANES spectra and (B) EXAFS spectra of Pd@Pt/PVP/C before and after the pre-reduction at 300 °C.

Table 2
Curve-fitting analysis of Pt L_3-Edge EXAFS of Pd@Pt/PVP/C.

Conditions	Shell	CN [a]	R /Å [b]	σ /Å [c]	R_f (%)[d]	k range/$Å^{-1}$ (R range/Å)	Number of free parameters
As-synthesized Pd@Pt/PVP/C	Cl	1.2 ± 0.95	2.09 ± 0.04	0.095 ± 0.07	9.0	3–16 (1.6–3.4)	12
	Pd	1.9 ± 0.70	2.72 ± 0.01	0.081 ± 0.05			
	Pt	4.6 ± 1.06	2.71 ± 0.01	0.081 ± 0.04			
Pd@Pt/PVP/C (after H_2 reduction)	Cl	0.97 ± 0.85	2.09 ± 0.05	0.098 ± 0.08	7.0		
	Pd	2.3 ± 0.58	2.73 ± 0.01	0.070 ± 0.04			
	Pt	4.7 ± 0.70	2.72 ± 0.01	0.082 ± 0.03			

[a] Coordination numbers.
[b] Bond distance.
[c] Debye-Waller factor.
[d] Residual factor.

Table 3
Catalyst screening for the Synthesis of 2,4,6 triphenyl pyrimidine from 1-phenyl ethanol, benzyl alcohol and benzamidine.

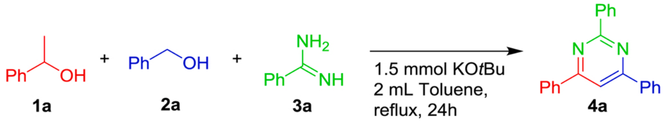

Entry	Pd (wt%)	Pt (wt%)	Cat. amount (mol%)	GC yield (%)
1	–	5	1	95
2	5	–	1	42
3	–	2.5	1	68
4	2.5	–	1	17
5[a]	2.5	2.5	0.5	81
6[b]	2.5	2.5	0.5	93
7[c]	2.5	2.5	0.5	84

[a] Pd@Pt/PVP/C prepared in batch process.
[b] Pd@Pt/PVP/C prepared in flow process (with 1.1 mmol KO*t*Bu).
[c] Pd@Pt/C prepared in flow process.

consisted of two atomic layers. Even after pre-reduction under a H_2 atmosphere at 300 °C, the core-shell structure is still stable and particle size is almost similar to fresh catalyst (Fig. S4) [79]. Table 1 shows Pt dispersion for the catalysts (pre-reduced at 300 °C) estimated by a standard CO chemisorption method. The result shows that 5 wt% Pt/C and 2.5 wt% Pd@Pt/PVP/C have similar Pt dispersion.

Fig. 2A shows the Pt L_3 edge XANES spectra of Pd@Pt/PVP/C before and after pre-reduction and Pt foil (reference compound for Pt metal). The peak height of the as-prepared Pd@Pt/PVP/C is slightly higher than that of Pt foil, and the reduction treatment decreased the peak height. This suggests that Pt species in the as-prepared Pd@Pt/PVP/C is a mixture of metallic Pt° as a main Pt species and a small amount of oxidized Pt species, which is converted to the metallic Pt° by the reduction treatment at 300 °C. As shown in Fig. 2B, the Fourier transforms of the EXAFS for the as-prepared and reduced Pd@Pt/PVP/C show significantly lower peak height for the Pt-Pt (and/or Pt-Pd) coordination than that for Pt foil, indicating that metal particle sizes of these samples are small. The EXAFS curve-fitting analysis (Table 2) of the as-prepared and reduced Pd@Pt/PVP/C shows the presence of Pt—Pt and Pt—Pd bonds with bond distance (2.71–2.73 Å) that is close to that of Pt foil (2.7X Å). Present fitting result at k/R space in Fig. S5. Since the coordination number of Pt–Pt shell (4.7) is adequately higher than that of

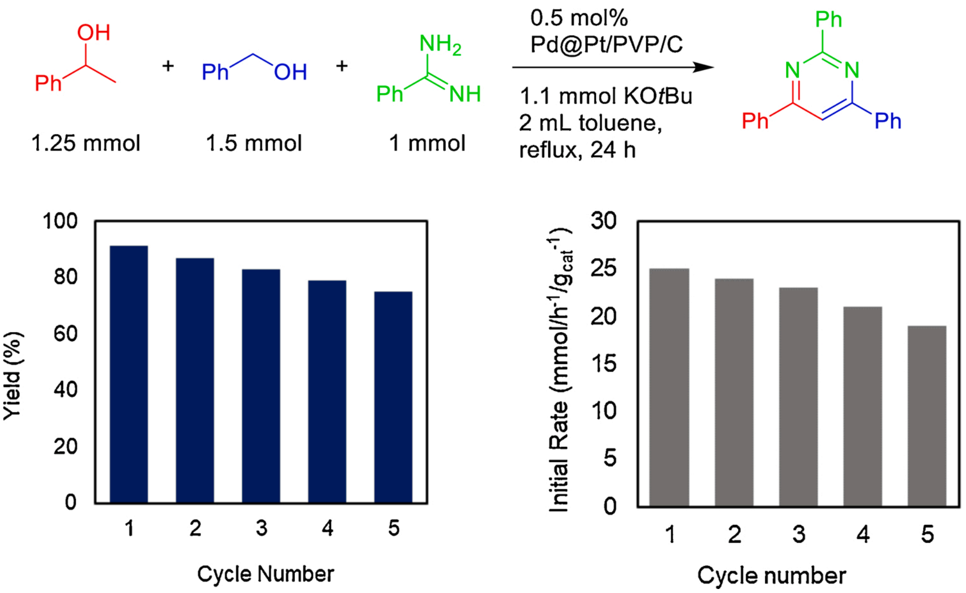

Fig. 3. Catalyst reuse for the synthesis promoted by Pd@Pt/PVP/C under the standard reaction conditions.

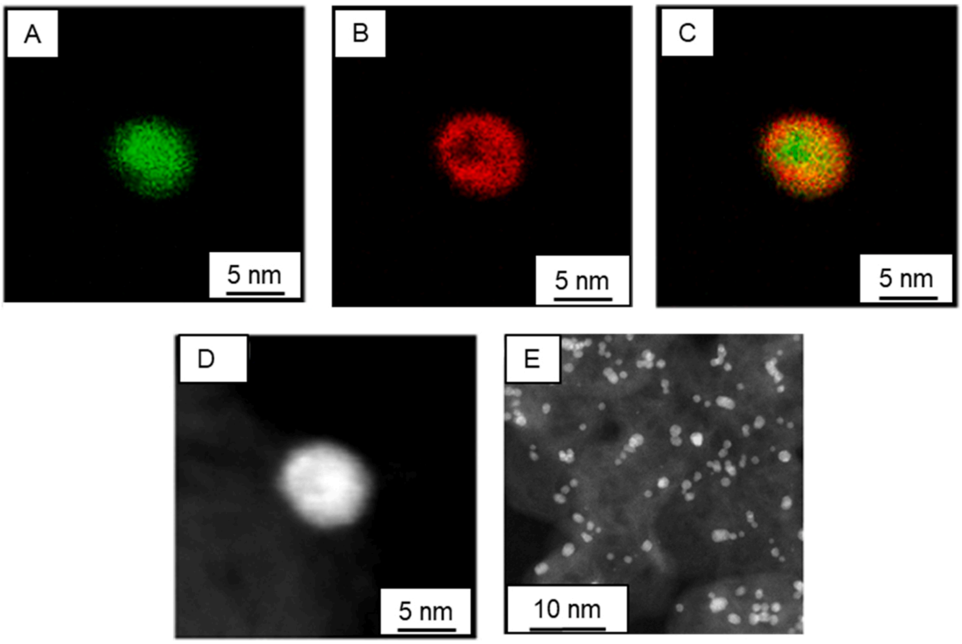

Fig. 4. DF-STEM-EDS mapping images (A-D), and DF-STEM image (E) with Pd shown in green and Pt in red, of Recycle-Pd@Pt/PVP/C NPs synthesized by the flow process.

Pt–Pd shell (2.3), Pd is supposed to be covered by Pt metal, giving the core-shell structure even after the H_2 treatment [80]. The result indicates that majority of Pt atoms are surrounded by Pt and a small part of Pt atoms are next to Pd atoms, and this local structure does not change after the reduction treatment. This EXAFS result is consistent with the Pd@Pt core-shell model observed by the DF-STEM-EDS mapping images. The small contribution of the Pt-Cl coordination suggests the presence of platinum chloride as a minor Pt species. The presence of the platinum chloride (oxidized Pt) species as a minor Pt species is consistent with the XANES result. Summarizing the XANES/EXAFS and DF-STEM-EDS results, it is shown that carbon-supported Pd@Pt core-shell metal nanoparticles are successfully prepared by the present flow reactor approach [79].

2.2. *Catalyst screening and reaction conditions*

Synthesis of 2,4,6-triphenyl pyrimidine by the reaction of 1-phenylethanol, benzyl alcohol and benzamidine [26] was investigated as a model reaction for the dehydrogenative cross-coupling of alcohols to form pyrimidines.

Table 3 shows the catalyst screening results for the synthesis of 2,4,6-triphenyl pyrimidines with the reaction of 1.25 mmol of 1-phenylethanol, 1.5 mmol of benzyl alcohol, and 1.0 mmol of benzamidine refluxing in toluene for 24 h. We compared various monometallic and bimetallic core-shell catalysts in the terms of the yield of the pyrimidine product based on benzamidine. The catalytic tests for the monometallic catalysts (Pt/C and Pd/C) were carried out using 1 mol% of the catalyst. Pt/C and Pd/C with metal content of 5 wt% show the pyrimidine yield of

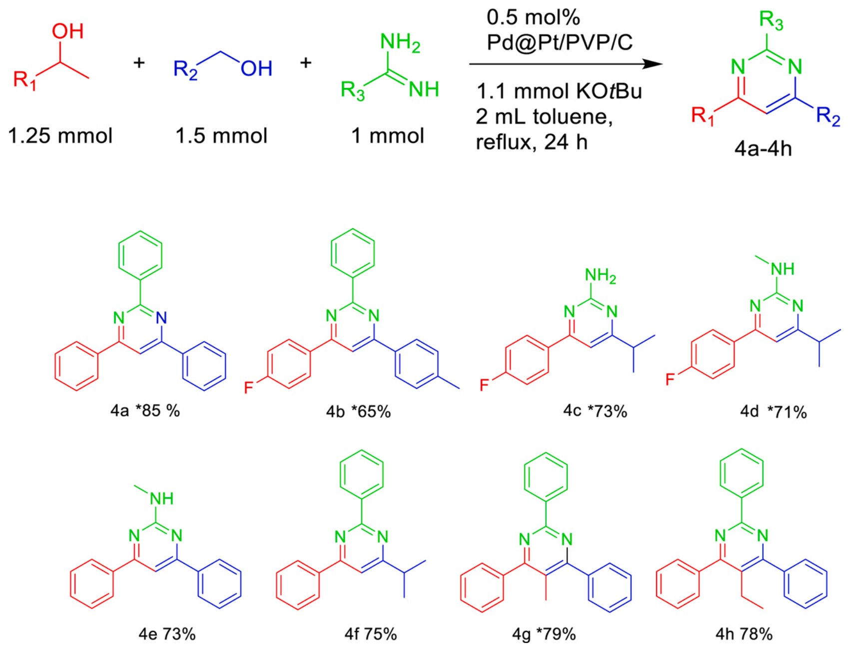

Scheme 2. Synthesis of pyrimidines from various secondary alcohols, primary alcohols and amidines. Isolated yields are shown.

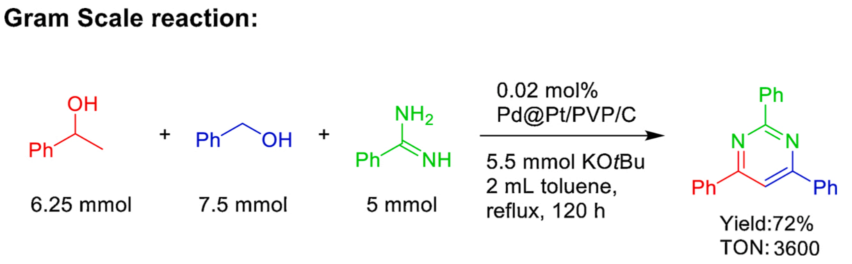

Scheme 3. Gram scale synthesis of pyrimidines from 1-phenyl ethanol, benzyl alcohol and benzamidine.

95% and 42%, respectively (entries 1–2), while Pt/C and Pd/C with metal content of 2.5 wt% showed lower yields of 68% and 17% (entries 3–4). The catalytic tests for the bimetallic catalysts (Pd@Pt/C, Pd@Pt/PVP/C) were carried out using 0.5 mol% of the catalyst. The reaction by 0.5 mol% core-shell Pd@Pt catalysts prepared by the flow process showed 93% yields (entry 6) comparable to the yield by 1 mol% Pt/C, suggesting that catalytic efficiency is improved by the presence of Pd core. The Pd@Pt catalyst prepared by a batch process (entry 5) showed lower yield than that prepared by the flow process (93%) (entry 6). The lower activity of former catalyst might be due to its larger metal particle size (about 5.0 nm). PVP is widely used as a capping agent that plays an important role to prevent the aggregation of nanoparticles [81,82]. The core-shell Pd@Pt catalyst without using PVP (entry 7) showed lower yield (84%) than that with PVP (93%).

It is well known that a bimetallic core-shell structure with an inner core of a metal and an external shell of another metal may provide unique physical and chemical properties [83,84]. In the Pd@Pt core-shell catalyst, Pt is slightly electron rich [85]. This might accelerate Pt-catalyzed C—H bond dissociation step as an important step of the present pyrimidine synthesis [26].

2.3. Recyclability test of Pd@Pt/PVP/C

Then, we tested the recyclability of this catalytic system (Fig. 3). After the standard reaction for 24 h, the catalysts were separated from the reaction mixture by centrifugation and dried at 40 °C for 3 h under vacuum, followed by the reduction in H_2 at 300 °C for 0.5 h. The recovered Pd@Pt/PVP/C catalyst showed high yield (93–78%) at least 5 cycles. The reaction rate slightly decreased during the recycle tests, which is consistent with the previously results for the recycle tests with Pt/C catalyst [26].

To investigate the possible reasons for the gradual catalyst deactivation, the recycled catalyst was characterized using DF-STEM (Fig. 4). The result revealed that the particles size for the recycled Pd@Pt/PVP/C catalyst (3.72 ± 0.73 nm) is close to that for the fresh catalyst (3.55 ± 0.62 nm) (Figs. S2 and S6). Comparison of the mapping images of the fresh (Fig. 1C) and recycled (Fig. 4C) catalyst shows that the core-shell structure is slightly changed by the reaction treatment, which can result in the slight decrease in the activity of the recycled catalyst. The reason of specific change is still unknown but one possibility is due to the slightly mixing of Pd and Pt during different treatments of the catalyst. It is noticed that the particle size of the NPs slightly increased during the recycle study. It might be the aggregation of NPs as it seems the secondary particles are slightly higher than primary particles.

2.4. Performance of Pd@Pt/PVP/C-catalyzed dehydrogenation reaction

Under the optimized reaction conditions, we studied the synthesis pyrimidines from various secondary alcohols, primary alcohols and amidines. As shown in Scheme 2, various primary alcohols including aromatic and aliphatic alcohols, 1-phenyl ethanol with different substituents at para-positions, and amidines were coupled to yield the corresponding pyrimidines (4a–4h) in good to high yields (65–93%). It should be noted that products 4c and 4d are important intermediates in

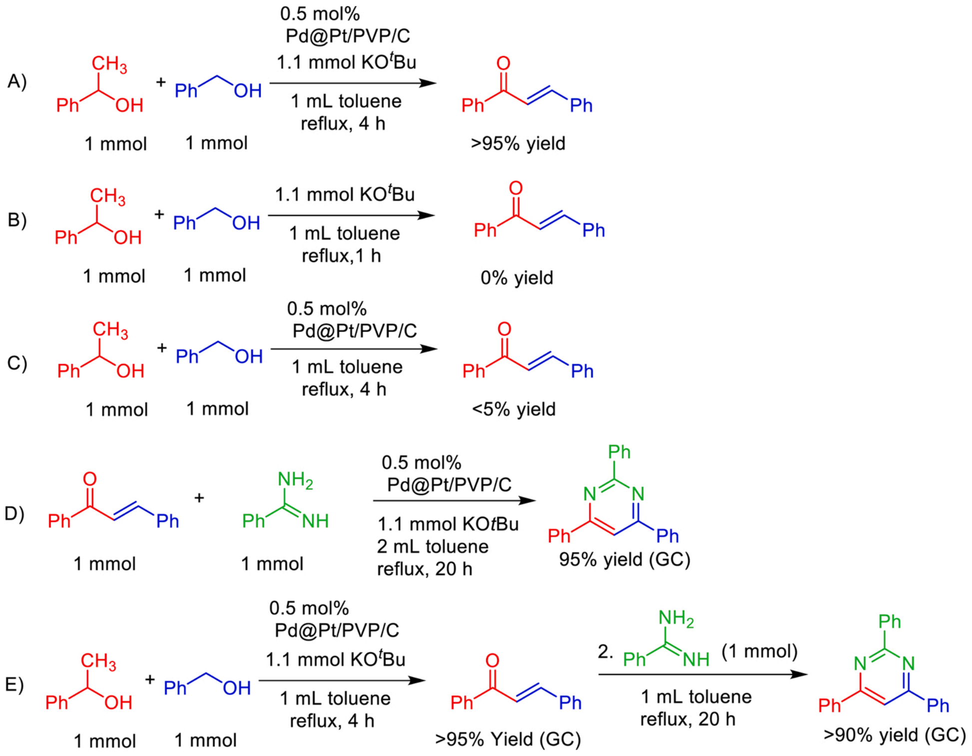

Scheme 4. Control experiments for the multicomponent synthesis of pyrimidines.

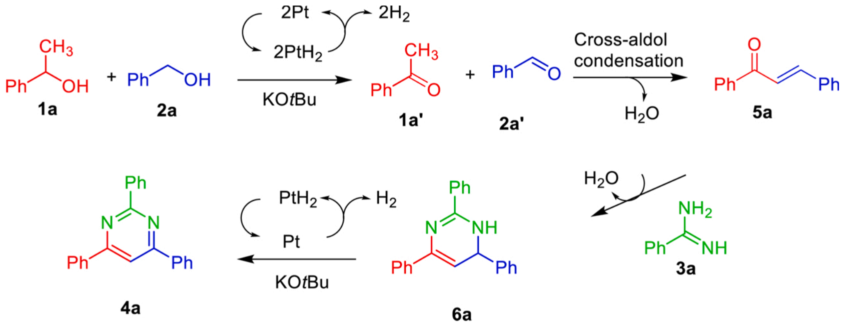

Scheme 5. Plausible reaction mechanism.

the total synthesis of rosuvastatin, which is used as a pharmaceutical drug for treatment of patients with high levels of cholesterol [26,86]. Notably, tetra-substituted pyrimidine derivatives were also synthesized in good yields by this protocol (4g and 4h).

The dehydrogenative synthesis of pyrimidine with alcohols and amidines with small amount of Pd@Pt/PVP/C (0.02 mol %) resulted in 72% yield of the product, corresponding to TON of 3600 (Scheme 3). This demonstrates the high catalytic efficiency of the present system.

2.5. Control experiment

Finally, we performed control experiments to explore the plausible reaction mechanism for the formation of 2,4,6-trisubstituted pyrimidines via selective C—C and C–N bond formation reaction catalyzed by Pd@Pt/PVP/C catalyst. First, the cross coupling of benzyl alcohol and 1-phenylethanol was carried out under the standard reaction conditions (Scheme 4A). The reaction for 4 h gave chalcone in >95% yield, whereas in the absence of catalyst, both alcohols remained unreacted (Scheme 4B). This result suggested that the dehydrogenation of alcohols was catalyzed by Pd@Pt/PVP/C where Pt sites acts as an active site of dehydrogenation and deprotonation steps of the reaction. In the absence of base, both alcohols reacted very slowly and produced 5% of chalcone (Scheme 4C), suggesting that base plays an important role such as deprotonation of alcohols and aldol condensation. The reaction of benzamidine with chalcone in the presence of catalyst and base gave the pyrimidine product in 95% yield (Scheme 4D). The reaction of chalcone, prepared by the reaction of benzyl alcohol and 1-phenylethanol (4h), with benzamidine gave the pyrimidine in 90% yield (Scheme 4E).

2.6. Reaction pathway

On the basis of control experiments and literature reports [26,50] a possible pathway for the formation of substituted pyrimidines is proposed in Scheme 5. The alcohols undergo dehydrogenation by a Pd@Pt core-shell catalyst to give ketone 1a' and aldehyde 2a', and molecular hydrogen. A subsequent base-mediated aldol condensation afford an α,β-unsaturated ketone intermediate 5a, which in turn reacts with the amidine to give intermediate 6a via intermolecular condensation. Finally, dehydrogenation of 6a produces the desired product 4a. The generation of 1a', 2a' and 5a was confirmed using GC–MS.

3. Conclusion

Carbon supported Pd@Pt core-shell bimetallic nanoparticle catalysts were successfully prepared by a flow reactor. The method is effective for continuous production of the supported core-shell catalysts with the precise control of nanoparticles particle size. The catalyst was effective for the one-pot synthesis of multi substituted pyrimidines from primary alcohols, secondary alcohols and amidines.

CRediT authorship contribution statement

Sharmin Sultana Poly, **Yuta Hashiguchi**, **Asima Sultana**, **Isao Nakamura**, **Ken-ichi Shimizu**, **Shunsaku Yasumura** and **Tadahiro Fujitani** contributed to this work.

Declaration of Competing Interest

The authors report no declarations of interest.

Acknowledgment

This work is based on results obtained from a project (JPNP16010) commissioned by the New Energy and Industrial Technology Development Organization (NEDO). The synchrotron radiation experiments were performed at the BL14B2 in SPring-8 with the approval of JASRI (No. 2017A1754, 2017B1782, 2017B1783, 2018A1764, 2018B1833, 2019A1782 and 2019B1872).

Appendix A. Supplementary data

Supplementary material related to this article can be found, in the online version, at doi:https://doi.org/10.1016/j.apcata.2021.118158.

References

[1] V. Sharma, N. Chitranshi, A.K. Agarwal, Int. J. Med. Chem. 2014 (2014) 202784–202815.
[2] M. Sahu, N. Siddiqui, Int. J. Pharm. Pharm. Sci 8 (2016) 8–21.
[3] G.G. Furin, Adv. Heterocycl. Chem. 42 (2006) 285–319.
[4] R. Singh, World J. Pharm. Pharm. Sci. 6 (2014) 124–127.
[5] A. Agarwal, K. Srivastava, S.K. Puri, P.M.S. Chauhan, Bioorg. Med. Chem. Lett. 15 (2005) 3133–3136.
[6] J.J. Fiol, M. Barceló-Oliver, A. Tasada, A. Frontera, À. Terrón, Á. García-Raso, Coord. Chem. Rev. 257 (2013) 2705–2715.
[7] M. Asif, Int. J. Bioorganic Chem. 2 (2017) 146–152.
[8] A.R. Katritzky, C.W. Rees, Comp. Heterocycl. Chem. 74 (1985), 233-233.
[9] J.M. Andersen, J.M. Dietschy, J. Biol. Chem. 253 (1978) 9024–9032.
[10] G. Joshi, H. Nayyar, J. Marin Alex, G.S. Vishwakarma, S. Mittal, R. Kumar, Curr. Top. Med. Chem. 16 (2016) 3175–3210.
[11] D.J. Brown, The Pyrimidines 139 (1962) 29–30.
[12] M. Johar, T. Manning, C. Tse, N. Desroches, B. Agrawal, D.Y. Kunimoto, R. Kumar, J. Med. Chem. 50 (2007) 3696–3705.
[13] N. Azas, P. Rathelot, S. Djekou, F. Delmas, A. Gellis, C. Di Giorgio, P. Vanelle, P. Timon-David, Farmaco 58 (2003) 1263–1270.
[14] N.A. Abdel-Latif, N.M. Sabry, A.M. Mohamed, M.M. Abdulla, Monatsh. Chem. 138 (2007) 715–724.
[15] A.G.E. Amr, A.M. Mohamed, S.F. Mohamed, N.A. Abdel-Hafez, A.E.F.G. Hammam, Bioorg. Med. Chem. 14 (2006) 5481–5488.
[16] N. Deibl, K. Ament, R. Kempe, J. Am. Chem. Soc. 137 (2015) 12804–12807.
[17] R. Mishra, I. Tomar, ChemInform. 2 (2011) 758–771.
[18] M. Bessières, V. Roy, L.A. Agrofoglio, RSC Adv. 4 (2014) 59747–59749.
[19] C.O. Tuck, E. Pérez, I.T. Horváth, R.A. Sheldon, M. Poliakoff, Science 337 (2012) 695–699.
[20] M.A.R. Meier, Macromol. Rapid Commun. 40 (2019) 1800524–1800534.
[21] S. Michlik, R. Kempe, Nat. Chem. 5 (2013) 140–144.
[22] M. Zhang, H. Neumann, M. Beller, Angew. Chemie - Int. Ed. 52 (2013) 597–601.
[23] S. Parua, S. Das, R. Sikari, S. Sinha, N.D. Paul, J. Org. Chem. 82 (2017) 7165–7175.
[24] C. Gunanathan, D. Milstein, Acc. Chem. Res. 44 (2011) 588–602.
[25] S.M.A. Hakim Siddiki, T. Toyao, K.I. Shimizu, Green Chem. 20 (2018) 2933–2952.
[26] S. Sultana Poly, S.M.A.H. Siddiki, A.S. Touchy, K.W. Ting, T. Toyao, Z. Maeno, Y. Kanda, K.I. Shimizu, ACS Catal. 8 (2018) 11330–11341.
[27] P. Daw, A. Kumar, N.A. Espinosa-Jalapa, Y. Diskin-Posner, Y. Ben-David, D. Milstein, ACS Catal. 8 (2018) 7734–7741.
[28] F. Li, L. Lu, P. Liu, Org. Lett. 18 (2016) 2580–2583.
[29] F. Li, C. Sun, N. Wang, J. Org. Chem. 79 (2014) 8031–8039.
[30] R. Wang, J. Ma, F. Li, J. Org. Chem. 80 (2015) 5737–5744.
[31] S. Parua, R. Sikari, S. Sinha, G. Chakraborty, R. Mondal, N.D. Paul, J. Org. Chem. 83 (2018) 11154–11166.
[32] N.A. Espinosa-Jalapa, A. Kumar, G. Leitus, Y. Diskin-Posner, D. Milstein, J. Am. Chem. Soc. 139 (2017) 11722–11725.
[33] M. Nielsen, H. Junge, A. Kammer, M. Beller, Angew. Chemie - Int. Ed. 51 (2012) 5711–5713.
[34] A. Khalafi-Nezhad, F. Panahi, ACS Catal. 4 (2014) 1686–1692.
[35] D. Srimani, Y. Ben-David, D. Milstein, Angew. Chemie - Int. Ed. 52 (2013) 4012–4015.
[36] R.H. Crabtree, Chem. Rev. 117 (2017) 9228–9246.
[37] P. Daw, Y. Ben-David, D. Milstein, J. Am. Chem. Soc. 140 (2018) 11931–11934.
[38] H.A. Ho, K. Manna, A.D. Sadow, Angew. Chemie - Int. Ed. 51 (2012) 8607–8610.
[39] N.D. Schley, G.E. Dobereiner, R.H. Crabtree, Organometallics 30 (2011) 4174–4179.
[40] D. Srimani, Y. Ben-David, D. Milstein, Chem. Commun. 49 (2013) 6632–6634.
[41] P. Daw, A. Kumar, N.A. Espinosa-Jalapa, Y. Ben-David, D. Milstein, J. Am. Chem. Soc. 141 (2019) 12202–12206.
[42] J. Zhu, H. Bienaymé, Multicomponent Reactions. 15 (2005), 2624-2624.
[43] R. Mondal, S. Sinha, S. Das, G. Chakraborty, N.D. Paul, Adv. Synth. Catal. 362 (2020) 594–600.
[44] S. Wang, N. Luo, Y. Li, C. Wang, Org. Lett. 21 (2019) 233–236.
[45] A.K. Bains, D. Adhikari, Catal. Sci. Technol. 9 (2019) 9051–9059.
[46] R. Mondal, I.B. Lozada, O. Stotska, D.E. Herbert, J. Org. Chem. 57 (2018) 4966–4978.
[47] N. Deibl, R. Kempe, Angew. Chemie - Int. Ed. 56 (2017) 1663–1666.
[48] M. Mastalir, M. Glatz, E. Pittenauer, G. Allmaier, K. Kirchner, J. Am. Chem. Soc. 138 (2016) 15543–15546.
[49] R. Mondal, D.E. Herbert, Organometallics 39 (2020) 1310–1317.
[50] M. Maji, S. Kundu, Dalton Trans. 48 (2019) 17479–17487.
[51] A.K. Bains, D. Adhikari, **10**, 2020, 6309-6318.
[52] Y. Lim, S.K. Kim, S.C. Lee, J. Choi, K.S. Nahm, S.J. Yoo, P. Kim, Nanoscale 6 (2014) 4038–4042.
[53] H. Zheng, M.S. Matseke, T.S. Munonde, Ultrason. Sonochem. 57 (2019) 166–171.
[54] H. Zhang, M. Jin, J. Wang, W. Li, P.H.C. Camargo, M.J. Kim, D. Yang, Z. Xie, Y. Xia, J. Am. Chem. Soc. 5 (2011) 8212–8222.
[55] J.W. Hong, S.W. Kang, B.S. Choi, D. Kim, S.B. Lee, S.W. Han, ACS Nano 6 (2012) 2410–2419.
[56] A.X. Yin, X.Q. Min, Y.W. Zhang, C.H. Yan, J. Am. Chem. Soc. 33 (2011) 3816–3819.
[57] A. Morlang, U. Neuhausen, K.V. Klementiev, F.W. Schütze, G. Miehe, H. Fuess, E. S. Lox, Appl. Catal. B Environ. 60 (2005) 191–199.
[58] G.W. Huber, J.W. Shabaker, S.T. Evans, J.A. Dumesic, Appl. Catal. B Environ. 43 (2006) 581–588.
[59] K. Tedsree, T. Li, S. Jones, C.W.A. Chan, K.M.K. Yu, P.A.J. Bagot, E.A. Marquis, G. D.W. Smith, S.C.E. Tsang, Nat. Nanotechnol. 6 (2011) 302–307.
[60] B. Lim, M. Jiang, P.H.C. Camargo, E.C. Cho, J. Tao, X. Lu, Y. Zhu, Y. Xia, Science 3 (2010) 69–80.
[61] R.S. Jayashree, J.S. Spendelow, J. Yeom, C. Rastogi, M.A. Shannon, P.J.A. Kenis, Electrochim. Acta 50 (2005) 4674–4682.
[62] H.A. Gasteiger, S.S. Kocha, B. Sompalli, F.T. Wagner, Appl. Catal. B Environ. 56 (2005) 9–35.
[63] S. Xie, S. Il Choi, N. Lu, L.T. Roling, J.A. Herron, L. Zhang, J. Park, J. Wang, M. J. Kim, Z. Xie, M. Mavrikakis, Y. Xia, Nano Lett. 14 (2014) 3570–3576.
[64] K.S. Siddiqi, A. Husen, Nanoscale Res. Lett. 11 (2016) 363–374.
[65] S. Il Choi, M. Shao, N. Lu, A. Ruditskiy, H.C. Peng, J. Park, S. Guerrero, J. Wang, M. J. Kim, Y. Xia, ACS Nano 8 (2014) 10363–10371.
[66] X. Auvray, L. Olsson, Appl. Catal. B Environ. 168 (2015) 1–578.
[67] T. Lopes, E. Antolini, E.R. Gonzalez, Int. J. Hydrogen Energy 33 (2008) 5563–5570.
[68] M. Miyakawa, N. Hiyoshi, H. Koda, K. Watanabe, H. Kunigami, H. Kunigami, A. Miyazawa, M. Nishioka, RSC Adv. 10 (2020) 6571–6575.
[69] A.S. Nair, B. Pathak, J. Phys. Chem. C 123 (2019) 3634–3644.
[70] D.A. Cantane, F.E.R. Oliveira, S.F. Santos, F.H.B. Lima, Appl. Catal. B Environ. 136–137 (2013) 351–360.
[71] K.J. Lin, L.J. Chen, M.R. Prasad, C.Y. Cheng, Adv. Mater. 16 (2004) 1845–1849.
[72] K.M. Koczkur, S. Mourdikoudis, L. Polavarapu, S.E. Skrabalak, Dalton Trans. 44 (2015) 17883–17905.
[73] K.M. Koczkur, S. Mourdikoudis, L. Polavarapu, Dalton Trans. 44 (2015) 17883–17905.
[74] M.B. Gawande, A. Goswami, T. Asefa, H. Guo, A.V. Biradar, D.L. Peng, R. Zboril, R. S. Varma, Chem. Soc. Rev. 44 (2015) 7540–7590.
[75] L. Wang, J. Luo, Q. Fan, M. Suzuki, I.S. Suzuki, M.H. Engelhard, Y. Lin, N. Kim, J. Q. Wang, C.J. Zhong, J. Phys. Chem. B 109 (2005) 21593–21601.

[76] V.S. Myers, M.G. Weir, E.V. Carino, D.F. Yancey, S. Pande, R.M. Crooks, Chem. Sci. 2 (2011) 1632–1646.
[77] S. Dutta, S. Sharma, A. Sharma, R.K. Sharma, ACS Omega 2 (2017) 2778–2791.
[78] Ö. Metin, S.F. Ho, C. Alp, H. Can, M.N. Mankin, M.S. Gültekin, M. Chi, S. Sun, Nano Res. 135 (2013) 16833–16836.
[79] Y.F. Nishimura, T. Hamaguchi, S. Yamaguchi, H. Takagi, K. Dohmae, T. Nonaka, Y. Nagai, J. Phys. Conf. Ser. 712 (2016) 012067–012072.
[80] A.I. Frenkel, Chem. Soc. Rev. 41 (2012) 8163–8178.
[81] S. Bhlapibul, K. Pruksathorn, P. Piumsomboon, Renew. Energy 41 (2012) 262–266.
[82] A.E. Yarulin, R.M. Crespo-Quesada, E.V. Egorova, L.L. Kiwi-Minsker, React. Kinet. Catal. 53 (2012) 253–261.
[83] F. Tao, M.E. Grass, Y. Zhang, D.R. Butcher, J.R. Renzas, Z. Liu, J.Y. Chung, B. S. Mun, M. Salmeron, G.A. Somorjai, Science 41 (2012) 7977–7979.
[84] H. Kobayashi, M. Yamauchi, H. Kitagawa, Y. Kubota, K. Kato, M. Takata, J. Am. Chem. Soc. 130 (2008) 1818–1819.
[85] S. Hayashi, R. Ishida, S. Hasegawa, S. Yamazoe, T. Tsukuda, Top. Catal. 54 (2018) 5915–5918.
[86] J.Y. Xu, W.H. Cheng, X. Zhu, H.L. Wu, K. Wang, Asian J. Chem. 5 (2008) 847–853.